ACS Chemical Neuroscience

Letter

pubs.acs.org/chemneuro

Novel Phenyl-Substituted 5,6-Dihydro-[1,2,4]triazolo[4,3-*a*]pyrazine P2X7 Antagonists with Robust Target Engagement in Rat Brain

Christa C. Chrovian,* Akinola Soyode-Johnson, Hong Ao, Genesis M. Bacani, Nicholas I. Carruthers, Brian Lord, Leslie Nguyen, Jason C. Rech, Qi Wang, Anindya Bhattacharya, and Michael A. Letavic

Janssen Research & Development, LLC, 3210 Merryfield Row, San Diego, California 92121-1126, United States

Supporting Information

ABSTRACT: Novel 5,6-dihydro-[1,2,4]triazolo[4,3-*a*]-pyrazine P2X7 antagonists were optimized to allow for good blood-brain barrier permeability and high P2X7 target engagement in the brain of rats. Compound **25** (huP2X7 IC_{50} = 9 nM; rat P2X7 IC_{50} = 42 nM) achieved 80% receptor occupancy for 6 h when dosed orally at 10 mg/kg in rats as measured by ex vivo radioligand binding autoradiography. Structure−activity relationships within this series are described, as well as in vitro ADME results. In vivo pharmacokinetic data for key compounds is also included.

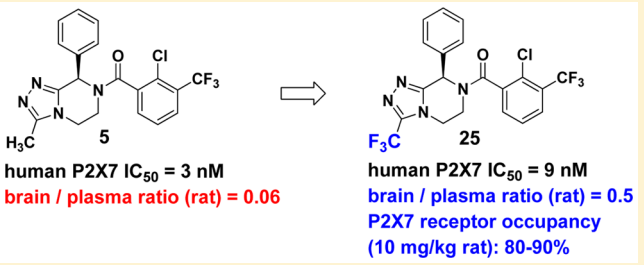

KEYWORDS: *P2X7, SAR, brain permeability, receptor occupancy, mood disorders*

P2X7 is a ligand gated ion channel expressed abundantly in CNS glial cells. It is known to be involved in an inflammatory cascade that results in the release of inflammatory cytokines, namely, IL-18 and IL-1β. Historical interest in this target has focused on attenuating the release of cytokines via P2X7 antagonism in inflammatory diseases such as rheumatoid arthritis (RA) and pain.[1−4] In the early 2000s, Pfizer[2] and AstraZeneca[3] progressed P2X7 antagonists into to Phase IIb studies for the treatment of RA. Although both compounds, CE-224,535 and AZD9056, were effective at blocking IL-1β release in patient plasma samples (after ex vivo stimulation with ATP and LPS), neither compound met desired clinical end points in RA.

More recent work has shown that P2X7 antagonists can mitigate neuroinflammatory responses in a number of conditions.[5] In one clinical example, GSK1482160 was administered in a Phase I trial with the intent of treating neuropathic and inflammatory pain.[6] This compound, like CE-224,535 and AZD9056, inhibited ex vivo IL-1β release in the study. However, due to its ability to cross the blood-brain barrier,[5−7] it would perhaps be better suited than CE-224,535 and AZD9056 to treat CNS disorders. Due to unsatisfactory safety margins, however, GSK1482160 was not further progressed.[6]

We became interested in P2X7 modulation as a potential treatment for psychiatric indications based on a number of reports that have identified a neuroinflammatory tone in the CNS of mood disorder patients.[8−11] There have also been reports of P2X7 knockout animals that exhibit a mood stabilizing phenotype,[11−14] and very recently, P2X7 antagonists have been shown to be efficacious in preclinical chronic models of depression.[11,15,16] We presented preliminary data suggesting that P2X7 antagonists that can cross the blood-brain barrier may be the most effective at treating psychiatric conditions.[16]

The 5,6-dihydro-[1,2,4]triazolo[4,3-*a*]pyrazine core has been established in the literature as drug-like[17] and is featured in a series of P2X7 antagonists.[18] We have previously published novel compounds composed of fused triazolo-ring systems that are potent brain penetrant P2X7 antagonists.[19,20] Many of these compounds, exemplified by **1** and **2**, have excellent human and rodent P2X7 potency. In addition, a number of compounds from these series were found to achieve high P2X7 receptor occupancy when measured 0.5 h after oral dosing. Our goal for this work was to achieve high receptor occupancy over a sustained period of time, in order to effectively interrupt the P2X7 inflammatory pathway.

During the course of our structure−activity relationship (SAR) studies, it was determined that the human P2X7 receptor tolerated 6-membered aliphatic carbocycle replacements for the aryl and heteroaryl groups off of these cores (**3**). However, reduction in ring size from cyclohexyl (**3**) to cyclopropyl (**4**) was not tolerated. We then found that activity could be revived with the cyclopropyl still in place, by introducing a phenyl group on the 8-position (**5**).

Keeping ligand efficiency (LE) in mind when embarking on a new chemical series,[21,22] efforts to further reduce molecular size were undertaken. It was found that when the phenyl group is introduced in the 8-position of these 5,6-dihydro-[1,2,4]-triazolo[4,3-*a*]pyrazin-7(8*H*)-yl)methanone cores, functionality

Special Issue: Neuroinflammation

Received: November 20, 2015
Accepted: January 11, 2016
Published: January 11, 2016

DOI: 10.1021/acschemneuro.5b00303
ACS Chem. Neurosci. 2016, 7, 490−497

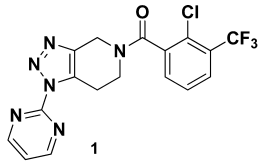

1

human P2X7 IC_{50} = 4.2 nM
rat P2X7 IC_{50} = 6.8 nM

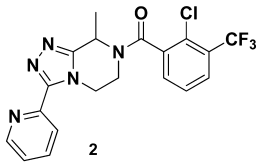

2

human P2X7 IC_{50} = 8.5 nM
rat P2X7 IC_{50} = 86 nM

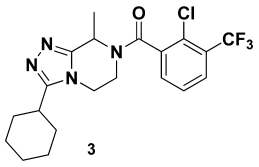

3

human P2X7 IC_{50} = 340 nM
rat P2X7 IC_{50} = >10,000 nM

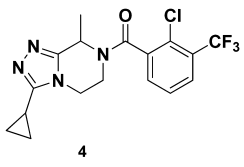

4

human P2X7 IC_{50} = >10,000 nM
rat P2X7 IC_{50} = >10,000 nM

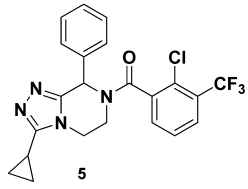

5

human P2X7 IC_{50} = 12 nM
rat P2X7 IC_{50} = 43 nM

as small as H in the 3-position could provide excellent human P2X7 activity (**6**; huP2X7 IC_{50} = 13 nM) as determined by a calcium mobilization assay in 1321N1 cells expressing the recombinant human P2X7 channel. A screen of a number of small groups on the 3-position of the core were prepared and tested (Table 1). Rat potency tended to improve with larger functionality at the 3-position; for example, compare compound **6** to both **7** and **5**. When the arene of the benzamide was removed, no activity remained up to 10 μM (**13**). Chiral HPLC separation of compound **5** indicated that P2X7 activity resides predominantly in a single enantiomer (**8**). We have tentatively assigned the active isomer as the R enantiomer (to be referred to as R*) based on data in our other core series and pharmacophore models.[19,23] Small carbocycles and an isopropanol group were found to be tolerated (**5**, **8**, **10**, and **12**). Aromatic groups were highly active at the human and rat receptors (**7**); however, these larger substituents were expected to result in compounds with molecular weights in excess of 500, after optimization of their physicochemical properties. For this reason they were generally not pursued in this series.

Compounds **5**−**12** were synthesized according to Scheme 1. A coupling of the commercially available acid chloride with Boc-protected ethylenediamine provided starting aminoamide **15** after deprotection. Compound **15** was cyclized to the phenyl-substituted piperazinone. Piperazinone **16** was then activated and cyclized to the 8-phenyl-5,6-dihydro-[1,2,4]-triazolo[4,3-*a*]pyrazines, which were elaborated to the final P2X7 antagonists.

The most promising compounds with potent in vitro human and rat P2X7 IC_{50} values from this series underwent further profiling for an in vitro assessment of ADME properties (microsomal stability, cytochrome P450 (CYP) inhibition, permeability, and plasma protein binding), solubility, and hERG channel inhibition (Table 2). Compounds **8** and **10** both

Table 1. In Vitro Antagonist Potency of 8-Phenyl-5,6-dihydro-[1,2,4]triazolo[4,3-*a*]pyrazin-7(8*H*)-yl)methanones in a Calcium Mobilization Assay[24]

Compd	Structure	huP2X7 IC_{50} (nM)	rP2X7 IC_{50} (nM)
6	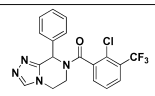	13±1.3	3065±1425
7	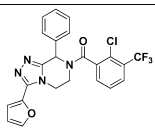	15 (n=1)	7 (n=1)
5	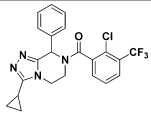	12±3	43±8
8	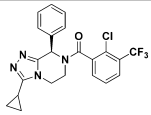	6.9±1.6	17±5
9	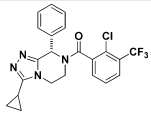	596±6	1035±64
10	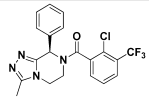	2.7±0.6	27±4
11	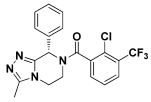	683±190	1594±392
12	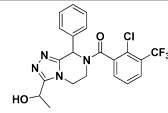	56±0.2	430±200
13	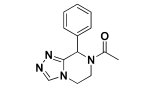	>10000	>10000

were stable in human and rat liver microsomes and demonstrated little or no inhibition of six CYP isoforms up to 10 μM, no hERG channel inhibition up to 10 μM, and good aqueous solubility. However, they were found to be substrates for *p*-glycoprotein (PGP) as measured in the Caco-2 human intestinal cell line assay, which measures the apical and basolateral flux of the substrate across the cell monolayer. PGP transporters are expressed in the apical membrane, and the permeability value is reported as ratio of its secretion (basolateral-to-apical velocity) to its absorption (apical-to-basolateral velocity).

Compound **10** was further evaluated for its ability to cross the blood-brain barrier in vivo. Brain levels of **10** were measured in rat after an oral dose of 10 mg/kg at multiple time points. The brain to plasma ratio at 30 min, 2 h, and 6 h ranged from 0.06 to 0.07 (203 ng/mL brain at 2 h). The low brain to plasma ratio is thought to be due to active efflux.

We next considered the possibility that the relatively basic 1,2,4-triazole may be contributing to the PGP liability of these compounds. Consequently we investigated functional groups in the 3-position that could influence the basicity of the triazole ring system, such as electron withdrawing groups or groups that

DOI: 10.1021/acschemneuro.5b00303
ACS Chem. Neurosci. 2016, 7, 490−497

Scheme 1. Synthesis of 8-Phenyl-5,6-dihydro-[1,2,4]triazolo[4,3-*a*]pyrazin-7(8*H*)-yl)methanones[a]

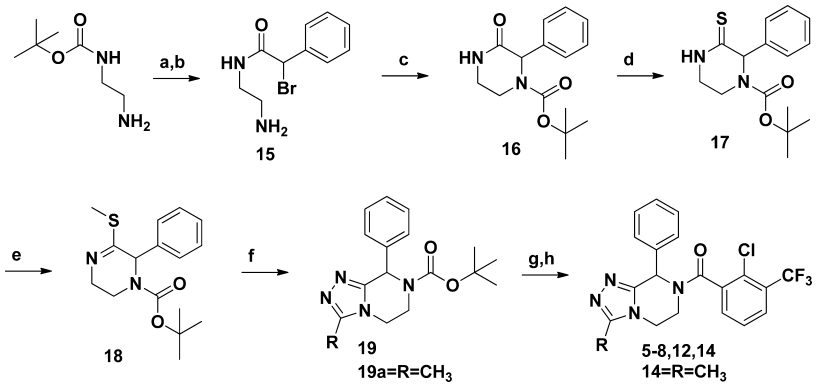

[a]Reagents and conditions: (a) 2-bromo-2-phenylacetyl chloride, NEt_3, CH_2Cl_2, 0 °C, 20 min (71%); (b) TFA, CH_2Cl_2, 16 h (99%); (c) K_2CO_3, THF, 65 °C, 16 h; then di-*tert*-butyldicarbonate, THF, 65 °C, 5 h (79%); (d) Lawesson's reagent, toluene, 110 °C, 3 h (23%); (e) iodomethane, acetonitrile, rt, 16 h; (f) *R*-hydrazide, *n*-butanol, 155 °C, 3 h; then di-*tert*-butyldicarbonate, rt, 1 h (43−63% over 2 steps); (g) TFA, CH_2Cl_2, rt; (h) 2-chloro-3-(trifluoromethyl)benzoyl chloride, NEt_3, CH_2Cl_2, 0 °C, 20 min (13%−66%).

Table 2. In Vitro ADME Data for Compounds 8 and 10

	10	8
hu/rat microsomal stability[a]	<0.3/<0.2	<0.3/0.21
CYP inhibition[b]	all >10 μM	all >10 μM except 2C8 = 9.6 μM
Caco-2 permeability[c]	5.10	3.33
hERG IC_{50}[d]	>10 μM	>10 μM
solubility pH 2/7	>400 μM/386 μM	198 μM/67 μM
hu/rat plasma proteins[e]	83.4/88.6	91.6/98.8

[a]Stability in human and rat liver microsomes. Data reported as extraction ratio. [b]CYP IC_{50} values were obtained from human liver microsomes for six isoforms: 1A2, 2C19, 2C8, 2C9, 2D6, and 3A4. [c]P_{app} is reported as B − A($\times10^{-6}$) cm/s/A − B($\times10^{-6}$) cm/s. [d]hERG IC_{50} (in μM) as measured in an [^{3}H]-dofetolide competition binding assay in HEK-293 cells expressing the hERG channel. [e]Plasma protein binding. Reported for human/rat as % bound.

possess steric bulk or ring strain. Several enantiopure compounds were prepared and their activity and Caco-2 ratios were measured. All of the compounds were highly active huP2X7 antagonists (IC_{50}'s < 20 nM, Table 3) and active rP2X7 antagonists (IC_{50}'s < 100 nM). Compounds containing R = H, or linear or branched hydrocarbon chains generally exhibited less desirable Caco-2 efflux ratios (**20**−**21**, **24**). Gratifyingly, the cyclobutyl, trifluoromethyl, and difluoromethyl functionalities showed good B → A/A → B ratios (<2) in the Caco-2 cell line and were poised for further investigation. Compounds **25** and **26** contain a $-CF_3$ and a $-CF_2H$ group, respectively, and are thought to be less susceptible to active transport due to the electron-withdrawing nature of the fluoromethyl groups.

Compounds **20**−**24** were synthesized according to Scheme 1 followed by chiral HPLC separation of enantiomers. Compounds **25**−**26** were synthesized by condensing the desired fluorinated anhydride onto the requisite hydrazine to form the unsaturated fused ring system (Scheme 2). The triazolopyrazine core could then be reduced using Pd/C, and elaborated to the final P2X7 antagonists.

Next, the structure−activity relationship of 8-phenyl replacements on 5,6-dihydro-[1,2,4]triazolo[4,3-*a*]pyrazin-7(8*H*)-yl)-methanones was investigated (Table 4). A para-fluorophenyl group was found to have human P2X7 potency for both the 3-

Table 3. In Vitro Antagonist Potency of and Caco-2 Data of 8*R-phenyl-5,6-dihydro-[1,2,4]triazolo[4,3-*a*]pyrazin-7(8*H*)-yl)methanones in a Calcium Mobilization Assay[14]**

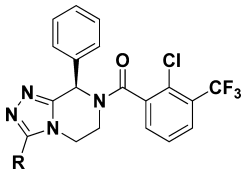

Compd	R	hP2X7 IC_{50} (nM)	rP2X7 IC_{50} (nM)	Caco-2 permeability[a]
20	**H**	4.5±1.6	64±11	4.50
10	**-CH_3**	2.7±0.6	27±4	5.10
21	**-CH_2CH_3**	2.4±0.7	59±13	3.24
22		10.2±1.4	168±31	ND
8		6.9±1.6	17±5	3.33
23		8.5±2.8	20±12	1.22
24		11±1.2	27±4	2.00
25	**-CF_3**	8.7±4.8	42±21	0.75
26	**-CF_2H**	8.8±1.9	82±13	0.78

[a]P_{app} is reported as B − A($\times10^{-6}$) cm/s/A − B($\times10^{-6}$) cm/s.

methyl and 3-cyclopropyl examples (**32** and **33**, respectively). However, in both of these cases, the rat potency was reduced compared to their desfluoro- parent compounds **8** and **10**. Pyridines and pyrazoles (**34**−**36**) were found to be more than 10-fold less potent than their phenyl parent compounds in human and >100-fold in rat. A benzyl group in the 8-position was tolerated at the human receptor but not the rat (**37**).

Compounds **23**, **25**, and **26** were profiled in vivo. The cyclobutyl compound **23**, despite good in vitro potency, was found to have low levels of P2X7 receptor occupancy as determined by an ex vivo radioligand binding autoradiography experiment in rat (Figure 1). The animal groups were dosed orally at 10 mg/kg and P2X7 receptor occupancy was determined at 0.5, 2, and 6 h. The brain and plasma levels revealed low brain levels of 76 ng/mL of **23** at 0.5 h, and a brain/plasma ratio of 0.05, likely contributing to the low observed level of receptor occupancy (Table 5). In vitro ADME

DOI: 10.1021/acschemneuro.5b00303
ACS Chem. Neurosci. 2016, 7, 490−497

Scheme 2. Synthesis of 3-Substituted $-CF_3$ and $-CF_2H$ Derivatives[a]

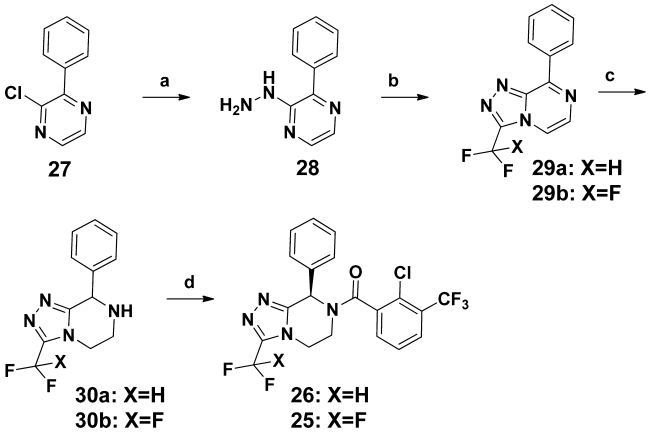

[a]Reagents and conditions: (a) $H_2NNH_2-H_2O$, 120 °C, 1 h (89%); (b) di- or trifluoroacetic anhydride, rt, 2 h; concentrate then add polyphosphoric acid, 140 °C, 16 h (57%–70%); (c) Pd/C, H_2, rt, 16 h (44–92%); (d) 2-chloro-3-(trifluoromethyl)benzoyl chloride; chiral HPLC (19–23% yield of desired enantiomer).

Table 4. In Vitro Antagonist Potency of Phenyl Replacement at the 8-Position of 5,6-Dihydro-[1,2,4]triazolo[4,3-*a*]pyrazin-7(8*H*)-yl)methanones

Compd	Structure	huP2X7 IC_{50} (nM)	rP2X7 IC_{50} (nM)
32	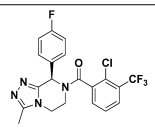	8.0±0.5	630±140
33	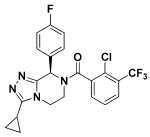	13 (n=1)	178 (n=1)
34	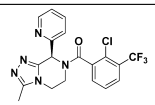	134 (n=1)	2825 (n=1)
35	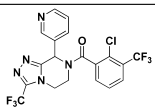	255 (n=1)	>10000 (n=1)
36	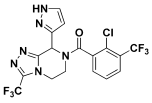	1540±10	>10000
37	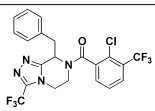	25±3.9	4530±2790

assays also revealed **23** to have moderate stability in liver microsomes and high plasma protein binding in rat (Table 5).

Compounds **25** and **26** both showed good brain penetration, achieving brain/plasma ratios of 0.5 (Table 6). Maximum P2X7 occupancies of 82% and 58% were measured at 10 mg/kg for **25** and **26**, respectively, in the ex vivo radioligand binding autoradiography experiment (Figure 1). The lower measured receptor occupancy for **26** vs **25** cannot be explained by comparing their brain levels or iv clearances (Table 5), in vitro

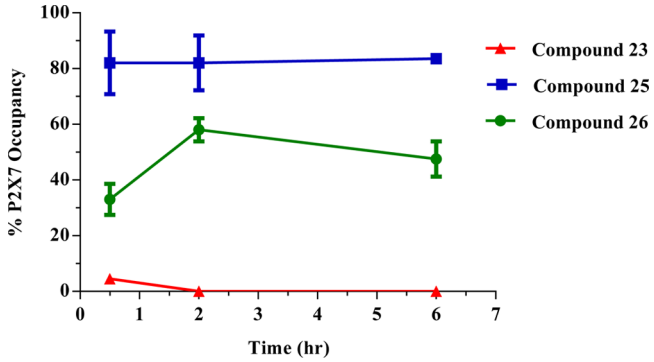

Figure 1. Ex vivo receptor occupancies of **23**, **25**, and **26** at 10 mg/kg dosed orally in rat.

rat K_i values or rat brain protein binding (Table 6). The values measured in these experiments are comparable between **25** and **26**. Both compounds also both showed good volumes of distribution and bioavailabilities (Table 5).

Examining the in vitro ADME and safety data (Table 6), **25** and **26** showed no CYP inhibition in six isoforms and no hERG channel inhibition. In an in vitro selectivity panel of 55 targets (CEREP ExpresSProfile), compound **25** showed little or no measurable inhibition of 45 receptors, 5 ion channels, and 3 transporters at 1 μM. It is of note that plasma free fraction for **25** was found to be about five times higher in human than in rat, and a similar variation was observed for **23**.

Compound **25** was investigated next in a dose response ex vivo radioligand binding autoradiography experiment (Figure 2). It was dosed orally as a suspension in 0.5% HPMC to rats at seven concentrations. Drug levels were measured after 2 h, and they were found to be dose-dependent in both the brain and plasma. The highest levels of ex vivo receptor occupancy measured was 90% at 10 mg/kg. The effective dose for 50% occupancy was 4.3 mg/kg, with a corresponding plasma EC_{50} of 748 ng/mL (total plasma concentration). Total brain levels at this dose were calculated to be 408 ng/mL. It is not known the degree of P2X7 blockade that will be efficacious in neuroinflammatory and psychiatric indications. Nonetheless, it is highly desirable to dose high enough in proof of concept studies to be able to achieve full receptor inhibition in a clinical setting. Based on plasma concentrations measured in the dose response receptor occupancy study, total plasma concentrations for 90% receptor occupancy would be approximately 2000 ng/mL in rat.

In conclusion, 8-phenyl substituted 5,6-dihydro-[1,2,4]-triazolo[4,3-*a*]pyrazin-7(8*H*)-yl)methanones are potent P2X7 antagonists. The substituent at the 3-position is an important determinant of both P2X7 rat potency and efflux propensity. We additionally found that fluorinated methyl groups significantly improved brain penetration compared to other small alkyl groups. Compounds **25** and **26** both showed good receptor occupancy at 10 mg/kg as determined by ex vivo autoradiography experiments in rat. Compound **25** had good brain/plasma levels and a linear dose-dependent response in the rat ex vivo receptor occupancy assay. From these studies, we calculated a high total plasma EC_{90} of approximately 2000 ng/mL in rat. Nonetheless, further study of **25** as a P2X7 antagonist is warranted.

DOI: 10.1021/acschemneuro.5b00303
ACS Chem. Neurosci. 2016, 7, 490–497

Table 5. Average Brain and Plasma Levels in Rats after a 10 mg/kg oral dose of 23, 25, or 26, and in Vivo Pharmacokinetic Data for 23, 25, and 26 in Rats (5 mg/kg Oral and 1 mk/kg iv Doses)[a]

	brain/plasma concn (ng/mL) 10 mg/kg				rat PK			
compd	0.5 h	2.0 h	6.0 h	B/P @ 2 h	iv Cl (mL/min/kg)	iv $T_{1/2}$ (h)	V_{ss} (L/kg)	F
23	76 ± 3/1288 ± 137	39 ± 11/848 ± 71	26 ± 16/745 ± 144	0.05	ND	ND	ND	ND
25	846 ± 317/1461 ± 341	881 ± 401/1618 ± 537	1162 ± 55/3034 ± 170	0.5	1.1	20.5	2.4	78%
26	927 ± 318/1502 ± 384	990 ± 313/2047 ± 438	792 ± 158/1549 ± 147	0.5	3.0	5.9	1.7	82%

[a]Brain (B) and plasma (P) concentrations listed in ng/mL.

Table 6. In Vitro ADME and Selectivity Data for 25, 26, and 23[a]

	25	26	23
rat K_i[b]	9.1 ± 4.0 nM	6.6 ± 3.1 nM	5.2 ± 1.8 nM
hu K_i[b]	11.9 ± 6.9 nM	4.1 ± 2.3 nM	10.2 ± 8.0 nM (n = 2)
hu/rat microsomal stability	<0.30/<0.20	<0.30/0.20	0.72/0.50
CYP inhibition	>10 μM	>10 μM	>10 μM
permeability (Caco-2)	0.75	0.78	1.2
hERG IC_{50}	>10 μM	>10 μM	>10 μM
solubility pH 2/7	22 μM/18 μM	38 μM/122 μM	100 μM/12 μM
hu/rat plasma proteins	92.0/98.6	90.7/91.1	96.9/99.4
rat brain proteins % bound	96.4	95.9	96.9

[a]See Table 2 for assay descriptions for microsomal stability, CYP inhibition, permeability, hERG, and plasma protein binding assays. [b]K_i values are reported as the mean of three experiments in triplicate, unless otherwise stated. hu is human, and r is rat. K_i ± sd is reported.

(a)

	Dose (mg/kg)						
	0.01	0.03	0.1	0.3	1.0	3.0	10.0
% P2X7 occupancy	0	0	0	0	9	29	90

(b)

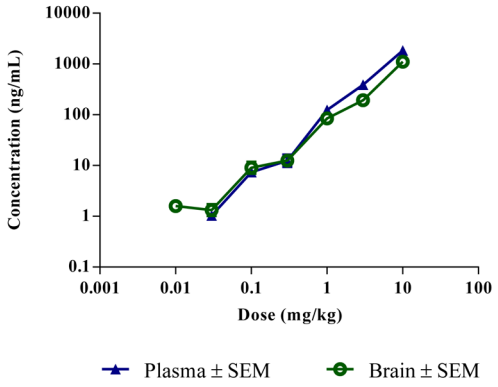

Figure 2. (a) Dose response analysis of the P2X7 antagonist **25** at 1 h in the ex vivo ligand binding autoradiography assay in rat. Receptor occupancy given the average % value of three animals per dose. (b) Corresponding brain and plasma concentrations for the P2X7 antagonist **25** at 1 h in rat in the dose response ex vivo ligand binding autoradiography assay. Concentrations shown are the average of n = 3 data points per dose.

METHODS

Chemistry. *Synthesis of **8** and **10**. tert-Butyl (2-(2-bromo-2-phenylacetamido)ethyl)carbamate.* A solution of *tert*-butyl *N*-(2-aminoethyl)carbamate (10 g, 59.29 mmol) in 40 mL of CH_2Cl_2 was cooled to −78 °C. Triethylamine (16.48 mL, 118.59 mmol) and 2-bromo-2-phenylacetyl chloride (13.85 g, 59.29 mmol) were subsequently added. The reaction was stirred for 20 min, warmed to 0 °C, and stirred for 1 h. The reaction was quenched with water and extracted three times with CH_2Cl_2. The combined organic layers were washed with brine, dried with $MgSO_4$, and concentrated. The resulting residue was purified via silica gel chromatography (0−50% ethyl acetate/hexanes) to provide the desired product (15.09 g, 71%) as a white solid. ^{1}H NMR (500 MHz, $CDCl_3$) δ 7.51−7.28 (m, 5H), 5.43−5.31 (m, 1H), 4.89 (s, 2H), 3.58−3.16 (m, 4H), 1.56−1.32 (m, 9H). MS (ESI) mass calcd. $C_{15}H_{21}BrN_2O_3$, 357.2; m/z found, 358.2 $[M + H]^+$.

*N-(2-Aminoethyl)-2-bromo-2-phenylacetamide (**15**).* To a solution of *tert*-butyl (2-(2-bromo-2-phenylacetamido)ethyl)carbamate (7.8 g, 21.75 mmol) in 30 mL of CH_2Cl_2 was added trifluoroacetic acid (16.6 mL, 217.49 mmol). The reaction was allowed to stir at room temperature overnight then concentrated and washed with satd. $NaHCO_3$ and extracted three times with CH_2Cl_2. The combined organic layers were dried using MgSO4, filtered, and concentrated to provide the desired product (10.54 g, 99%). MS (ESI) mass calcd. $C_{10}H_{13}BrN_2O$, 257.2; m/z found, 258.2 $[M + H]^+$.

*tert-Butyl 3-oxo-2-phenylpiperazine-1-carboxylate (**16**).* To a solution of **15** (19.28 g, 43.74 mmol) in 430 mL of THF was added anhydrous K_2CO_3 (60.46 g, 437.46 mmol). The reaction was refluxed at 65 °C overnight. Di-*tert*-butyldicarbonate (19.28 g, 87.49 mmol) was then added, and the reaction was refluxed at 65 °C for an additional 5 h and then cooled to room temperature, diluted with ethyl acetate, and washed with water. The organic layer was partitioned, dried with $MgSO_4$, filtered, concentrated, and purified via silica gel chromatography (0−30% ethyl acetate/hexanes) to provide the desired product (9.54 g, 79%) as a white solid. ^{1}H NMR (500 MHz, $CDCl_3$) δ 7.42−7.27 (m, 5H), 6.02−5.71 (m, 1H), 4.15−4.06 (m, 1H), 3.80−3.69 (m, 1H), 3.69−3.61 (m, 1H), 3.42−3.30 (m, 1H), 1.51 (s, 9H). MS (ESI) mass calcd. $C_{15}H_{20}N_2O_3$, 276.3; m/z found, 277.2 $[M + H]^+$.

*tert-Butyl 2-phenyl-3-thioxopiperazine-1-carboxylate (**17**).* To a mixture of Lawesson's reagent (4.15 g, 9.95 mmol) in 125 mL of toluene was added **16** (2.5 g, 9.05 mmol) in toluene (approx. 10 mL). The mixture was heated at 110 °C for 3 h in a sealed tube. The reaction was worked up with 10% NaOH and extracted three times with ethyl acetate. The combined organic layers were dried with $MgSO_4$, filtered, concentrated, and purified via silica gel chromatography (0−50% ethyl acetate/hexanes) to provide the desired product (614 mg, 23%) as a crystalline orange solid. ^{1}H NMR (500 MHz, $CDCl_3$) δ 9.67 (s, 1H), 7.51−7.41 (m, 2H), 7.37−7.27 (m, 3H), 6.13 (s, 1H), 4.08−3.77 (m, 1H), 3.53−3.38 (m, 1H), 3.38−3.26 (m, 2H), 1.50 (s, 9H). ^{13}C NMR (101 MHz, $CDCl_3$) δ 199.5, 153.5, 138.7, 128.6, 128.1, 127.5, 81.4, 65.5, 43.1, 36.1, 28.4. MS (ESI) mass calcd. $C_{15}H_{20}N_2SO_2$, 292.1; m/z found, 293.2 $[M + H]^+$.

*tert-Butyl 3-(methylthio)-2-phenyl-5,6-dihydropyrazine-1(2H)-carboxylate (**18**).* To a stirred solution of **17** (390 mg, 1.33 mmol)) in 3 mL of acetonitrile was added iodomethane (227 mg, 1.60 mmol). The reaction was stirred at room temperature overnight and then concentrated to provide the desired product (407 mg, 99%). ^{1}H NMR (500 MHz, $CDCl_3$) δ 7.51−7.41 (m, 3H), 7.40−7.31 (m, 2H), 6.17 (s, 1H), 4.25−4.08 (m, 2H), 4.06−3.90 (m, 1H), 3.50−3.37 (m, 1H),

DOI: 10.1021/acschemneuro.5b00303
ACS Chem. Neurosci. 2016, 7, 490−497

3.08 (s, 3H), 1.48 (s, 9H). MS (ESI) mass calcd. $C_{16}H_{22}N_2SO_2$, 306.1; m/z found, 307.2 $[M + H]^+$.

*tert-Butyl 3-methyl-8-phenyl-5,6-dihydro-[1,2,4]triazolo[4,3-a]-pyrazine-7(8H)-carboxylate (**19a**).* To a round-bottom flask was added **18** (606 mg, 1.978 mmol), acetic hydrazide (1.48 g, 19.76 mmol) followed by 10 mL of *n*-butanol. The reaction was heated to 155 °C and stirred for 3 h then cooled to room temperature and di-*tert*-butyl dicarbonate (436 mg, 1.978 mmol) was added. The reaction was subsequently stirred for 1 h at room temperature and then isolated, concentrated, and purified via silica gel chromatography (0−10% 2 M NH_3-MeOH/CH_2Cl_2) to produce the desired product (390 mg, 63%). ^{1}H NMR (400 MHz, $CDCl_3$) δ 7.40−7.20 (m, 5H), 6.67 (s, 1H), 4.45 (s, 1H), 3.98−3.77 (m, 2H), 3.32−3.16 (m, 1H), 2.44 (s, 3H), 1.54−1.48 (m, 9H). MS (ESI) mass calcd. $C_{17}H_{22}N_4O_2$, 314.2; m/z found, 315.0 $[M + H]^+$.

*(2-Chloro-3-(trifluoromethyl)phenyl)(3-methyl-8-phenyl-5,6-dihydro-[1,2,4]triazolo[4,3-a]pyrazin-7(8H)-yl)methanone (**14**).* To a solution of **19a** (390 mg, 1.24 mmol) in 5 mL of CH_2Cl_2 was added trifluoroacetic acid (0.390 mL, 5.10 mmol). The reaction was allowed to stir at room temperature overnight and then concentrated, washed with conc. $NaHCO_3$, and extracted three times with CH_2Cl_2. The combined organic layers were dried using $MgSO_4$, filtered, and concentrated to give 3-methyl-8-phenyl-5,6,7,8-tetrahydro-[1,2,4]-triazolo[4,3-*a*]pyrazine. ^{1}H NMR (400 MHz, $CDCl_3$) δ 7.42−7.37 (m, 2H), 7.36−7.26 (m, 3H), 5.22 (s, 1H), 3.92−3.80 (m, 2H), 3.36−3.27 (m, 1H), 3.24−3.16 (m, 1H), 2.39 (s, 3H), 2.36 (2, 1H). ^{13}C NMR (101 MHz, $CDCl_3$) δ 151.4, 150.0, 139.3, 128.6, 128.13, 128.08, 57.0, 42.9, 40.6, 10.2. MS (ESI) mass calcd. $C_{12}H_{14}N_4$, 214.27; m/z found, 215.0 $[M + H]^+$. The crude compound was dissolved in 5 mL of CH_2Cl_2, and triethylamine was added (0.234 mL, 1.68 mmol). The reaction was stirred for 5 min at room temperature and then cooled to 0 °C. 2-Chloro-3-(trifluoromethyl)benzoyl chloride (272 mg, 1.120 mmol) was added, and the reaction was stirred at 0 °C for 20 min. The reaction was quenched with water, warmed to room temperature, and extracted three times with CH_2Cl_2. The combined organic layers were dried using $MgSO_4$, concentrated, and purified via basic HPLC (Agilent prep system, Waters XBridge C18 5 μm 50 × 150 mm column, 5−95% MeCN/20 mM NH_4OH over 22 min at 80 mL/min) to provide the racemic product (157 mg, 30%). ^{1}H NMR (500 MHz, $CDCl_3$) δ 7.87−7.70 (m, 1H), 7.60−7.29 (m, 7H), 6.21−5.93; 5.21−5.01 (series of m, 1H), 4.16−3.30 (series of m, 4H), 2.51−2.45 (m, 3H). MS (ESI): mass calcd. for $C_{20}H_{16}ClF_3N_4O$+H, 421.1037; m/z found, 421.1055 $[M + H]^+$.

*(2-Chloro-3-(trifluoromethyl)phenyl)(3-methyl-8-phenyl-5,6-dihydro-[1,2,4]triazolo[4,3-a]pyrazin-7(8H)-yl)methanone (**10**).* Compound **14** (222 mg, 0.528 mmol) was separated via chiral SFC (stationary phase: CHIRALPAK AD-H 5 μm 250 × 20 mm, mobile phase: 70% CO_2, 30% iPrOH), yielding the desired product (98 mg, 44%) as a mixture of several rotamers. ^{1}H NMR (500 MHz, $CDCl_3$) δ 7.87−7.70 (m, 1H), 7.60−7.29 (m, 7H), 6.21−5.93; 5.21−5.01 (series of m, 1H), 4.16−3.30 (series of m, 4H), 2.51−2.45 (m, 3H). For the major rotamer: ^{13}C NMR (151 MHz, DMSO) δ 165.6, 150.1, 147.9, 137.3, 137.0, 132.0, 128.7, 128.63, 128.60, 128.1, 127.1, 125.3, 123.5, 121.7, 119.9, 50.9, 41.4, 9.6. MS (ESI): mass calcd. for $C_{20}H_{16}ClF_3N_4O$+H, 421.1037; m/z found, 421.1051 $[M + H]^+$. The enantiomeric ratio was determined to be 100% by chiral SFC analysis (Chiralpak AD, 30% iPrOH + (0.3% $iPrNH_2$), 35 °C, 3 mL/min), t_R(major) = 3.45 min, t_R (minor) = 5.32 min. $[\alpha]_D^{20}$ = −82.8 (c = 0.344, MeOH).

*(2-Chloro-3-(trifluoromethyl)phenyl)(3-cyclopropyl-8-phenyl-5,6-dihydro-[1,2,4]triazolo[4,3-a]pyrazin-7(8H)-yl)methanone (**8**).* The desired product was prepared in an analogous manner to compound **14** (using cyclopropanecarbohydrazide instead of acetic hydrazide to form **19**). The intermediate used in the final coupling step, 3-cyclopropyl-8-phenyl-5,6,7,8-tetrahydro-[1,2,4]triazolo[4,3-*a*]pyrazine, was characterized: ^{1}H NMR (400 MHz, $CDCl_3$) δ 7.41−7.35 (m, 2H), 7.34−7.23 (m, 3H), 5.21 (s, 1H), 4.02−3.90 (m, 2H), 3.32−3.23 (m, 1H), 3.22−3.12 (m, 1H), 2.32 (s, 1H), 1.75−1.63 (m, 1H), 1.13−1.06 (m, 2H), 1.04−0.94 (m, 2H). ^{13}C NMR (101 MHz, CDCl3) δ 154.9, 151.2, 139.4, 128.5, 128.1, 128.0, 56.7, 42.9, 40.3, 6.6, 6.4, 5.0. MS (ESI) mass calcd. $C_{14}H_{16}N_4$, 240.31: m/z found, 241.2 $[M + H]^+$. The enantiomers of compound **5** were separated via chiral SFC (stationary phase: CHIRALPAK AD-H 5 μm 250 × 20 mm; mobile phase: 70% CO_2, 30% iPrOH) yielding the desired product as a mixture of several rotamers. ^{1}H NMR (400 MHz, $CDCl_3$) δ 7.86−7.71 (m, 1H), 7.60−7.29 (m, 7H), 6.15−5.99; 5.20−5.02 (series of m, 1H), 4.25−3.30 (series of m, 4H), 1.78−1.68 (m, 1H), 1.28−1.16 (m, 2H), 1.16−0.99 (m, 2H). For the major rotamer: ^{13}C NMR (151 MHz, DMSO) δ 165.5, 154.6, 147.8, 137.2, 137.0, 132.1, 128.7, 128.6, 128.5, 127.1, 125.3, 123.4, 121.6, 120.0, 50.8, 41.4, 6.6, 6.1, 4.4. MS (ESI) mass calcd. $C_{22}H_{18}ClF_3N_4O$+H, 447.1194; m/z found, 447.1190 $[M + H]^+$. The enantiomeric ratio was determined to be 100% by chiral SFC analysis (Chiralpak AD, 30% iPrOH + (0.3% $iPrNH_2$), 35 °C, 3 mL/min), t_R (major) = 4.08 min, t_R (minor) = 4.89 min.

*Synthesis of **25** and **26**. 2-Chloro-3-phenylpyrazine (**27**).* To a solution of 2,3-dichloropyrazine (1.50 g, 10.07 mmol) and phenylboronic acid (1.23 g, 10.07 mmol) in 35 mL of DME was added Na_2CO_3 (1.07 g, 10.07 mmol) in 15 mL of water. N_2 gas was bubbled through the reaction mixture for 15 min then the flask was equipped with a condenser and purged with N_2 for another 15 in before adding tetrakis(triphenylphosphine)palladium (582 mg, 0.503 mmol). The reaction was heated to reflux and allowed to stir overnight. The reaction was cooled to rt, diluted with 80 mL of water, and extracted three times with CH_2Cl_2. The combined organic extracts were dried with $MgSO_4$, filtered, concentrated, and purified via silica gel chromatography (0−30% ethyl acetate/hexanes) to provide the desired product (1.39 g, 72%) as a white solid. MS (ESI) mass calcd. $C_{10}H_7ClN_2$, 190.0; m/z found, 191.0 $[M + H]^+$.

*2-Hydrazinyl-3-phenylpyrazine (**28**).* A neat suspension of **27** (1.39 g, 7.23 mmol) in hydrazine monohydrate (3.6 mL, 72.78 mmol) was placed in microwave vial and irradiated at 120 °C for 1 h. The resulting reaction mixture was cooled down to rt, diluted with 30 mL water, and extracted three times with 30 mL of CH_2Cl_2. The combined organic extracts were dried using $MgSO_4$ and concentrated under reduced pressure to provide the desired product (1.21 g, 89%). MS (ESI) mass calcd. $C_{10}H_{10}N_4$, 186.1; m/z found, 187.2 $[M + H]^+$.

*3-(Difluoromethyl)-8-phenyl-[1,2,4]triazolo[4,3-a]pyrazine (**29**).* A neat residue of **28** (665 mg, 3.57 mmol) was cooled to 0 °C and difluoroacetic anhydride (4.44 mL, 35.7 mmol) was added dropwise. The reaction was allowed to stir at room temperature for 2 h then concentrated. The residue was suspended in 4 mL of polyphosphoric acid to form a gelatinous mixture, which was heated to 140 °C and stirred overnight. The reaction was neutralized to pH 7 with NaOH pellets and ice water. The resulting aqueous solution was extracted three times with ethyl acetate. The combined organic extracts were dried with $MgSO_4$, concentrated, and purified via silica gel chromatography (0−50% ethyl acetate/hexanes) to provide the desired product (500 mg, 57%). ^{1}H NMR (500 MHz, $CDCl_3$) δ 8.84−8.77 (m, 2H), 8.20 (d, J = 4.6 Hz, 1H), 8.12 (d, J = 4.6 Hz, 1H), 7.60−7.53 (m, 3H), 7.45−7.22 (m, 1H). MS (ESI) mass calcd. $C_{12}H_8F_2N_4$, 246.1; m/z found, 247.1 $[M + H]^+$.

*3-(Difluoromethyl)-8-phenyl-5,6,7,8-tetrahydro-[1,2,4]triazolo-[4,3-a]pyrazine (**30a**).* To a round-bottom flask containing a solution of **29** (500 mg, 2.03 mmol) in 5 mL ethanol was added 10% palladium on carbon (wet Degussa powder, 108 mg, 0.102 mmol). The reaction vessel was purged with N_2 gas, fitted with a hydrogen balloon (1 atm), and stirred at rt overnight. The reaction mixture was then filtered through a pad of Celite, and the filtrate was concentrated under reduced pressure to provide the desired product (470 mg, 92%). MS (ESI) mass calcd. $C_{12}H_{12}F_2N_4$, 250.1; m/z found, 251.1 $[M + H]^+$.

*(2-Chloro-3-(trifluoromethyl)phenyl)(3-(difluoromethyl)-8-phenyl-5,6-dihydro-[1,2,4]triazolo[4,3-a]pyrazin-7(8H)-yl)methanone (**26**).* To a solution of **30** (150 mg, 0.60 mmol) in 5 mL of CH_2Cl_2 was added triethylamine (0.25 mL, 1.8 mmol). The reaction was stirred for 5 min at room temperature and then cooled to 0 °C. 2-Chloro-3-(trifluoromethyl)benzoyl chloride (291 mg, 1.20 mmol) was added and the reaction was stirred at 0 °C for 20 min. The reaction was quenched with water and warmed to room temperature then extracted three times with CH_2Cl_2. The combined organic layers were dried using $MgSO_4$, concentrated, and purified via basic HPLC to provide

DOI: 10.1021/acschemneuro.5b00303
ACS Chem. Neurosci. 2016, 7, 490−497

the racemate (132 mg, 48%). The racemate was separated via chiral SFC (stationary phase: CHIRALPAK AD-H 5um 250 × 20 mm; mobile phase: 70% CO_2, 30% iPrOH) yielding the desired product as a mixture of several rotamers (63 mg, 23% overall yield). ^{1}H NMR (400 MHz, $CDCl_3$) δ 7.87−7.77 (m, 1H), 7.61−7.32 (m, 7H), 7.14−6.84 (m, 1H), 6.29−6.08; 5.17−5.10 (series of m, 1H), 4.43−3.27 (series of m, 4H). For the major rotamer: ^{13}C NMR (126 MHz, DMSO) δ 165.6, 150.7, 146.5, 137.2, 136.5, 132.2, 128.9, 128.7, 128.4, 127.2, 125.9, 123.7, 121.5, 119.3, 110.7, 108.8, 106.9, 50.9, 42.9. MS (ESI) mass calcd. $C_{20}H_{14}ClF_5N_4O$ + H, 457.0849; m/z found, 457.0832 $[M + H]^+$. The enantiomeric ratio was determined to be 100% by chiral SFC analysis (Chiralpak AD, 30% iPrOH+(0.3% $iPrNH_2$), 35 °C, 3 mL/min), t_R (major) = 2.08 min, t_R (minor) = 3.41 min. $[\alpha]_D^{20}$ = −87.8 (c = 0.319, MeOH).

*3-(Trifluoromethyl)-8-phenyl-5,6,7,8-tetrahydro-[1,2,4]triazolo-[4,3-a]pyrazine (**30b**).* The desired product was prepared in an analogous manner to **30a** (using trifluoracetic anhydride instead of difluoroacetic anhydride to form **29**). ^{1}H NMR (500 MHz, $CDCl_3$) δ 7.44−7.31 (m, 5H), 5.34 (s, 1H), 4.20−4.15 (m, 2H), 3.44−3.37 (m, 1H), 3.32−3.25 (m, 1H), 2.16 (br s, 1H). ^{13}C NMR (126 MHz, $CDCl_3$) δ 154.2, 144.1, 143.8, 143.5, 143.2, 138.2, 128.8, 128.6, 128.0, 57.1, 44.7, 44.7, 40.4.

*(2-Chloro-3-(trifluoromethyl)phenyl)(8-phenyl-3-(trifluoromethyl)-5,6-dihydro-[1,2,4]triazolo[4,3-a]pyrazin-7(8H)-yl)methanone (**25**).* The desired product was prepared in an analogous manner to **26**. The racemate was separated via chiral SFC (stationary phase: CHIRALPAK AD-H 5 μm 250 × 20 mm; mobile phase: 80% CO_2, 20% iPrOH) yielding the desired product as a mixture of several rotamers. ^{1}H NMR (400 MHz, $CDCl_3$) δ 7.86−7.77 (m, 1H), 7.60−7.32 (m, 7H), 6.26−6.08; 5.23−5.09 (m, 1H), 4.40−3.36 (m, 4H). For the major rotamer: ^{13}C NMR (151 MHz, DMSO) δ 165.5, 151.6, 143.2, 142.9, 142.7, 142.4, 137.0, 136.2, 132.2, 128.85, 128.79, 128.74, 128.72, 128.4, 127.3, 125.3, 123.5, 121.7, 121.1, 119.8, 119.3, 117.5, 115.7, 50.9, 43.6, 39.0. MS (ESI) mass calcd. $C_{20}H_{13}ClF_6N_4O$ + H, 475.0755; m/z found, 475.0762 $[M + H]^+$. The enantiomeric purity was determined to be 100% by chiral SFC analysis (Chiralpak AD, 20% iPrOH + (0.3% $iPrNH_2$), 35 °C, 3 mL/min), t_R (major) = 2.76 min, t_R (minor) = 3.91 min. $[\alpha]_D^{25}$ = −84.1 (c = 0.607, MeOH).

Pharmacological Assays. *Primary Pharmacological Assays.* Lipopolysaccharide (LPS)-primed, Bz-ATP induced IL-1β release from human peripheral blood mononuclear cells (PBMC) was used as the primary screen to test for P2X7 antagonism and was conducted as previously described.[25,26]

P2X7 ex Vivo Radioligand Binding Autoradiography. Animal work was done in accordance with the Guide Care for and Use of Laboratory Animals adopted by the United States National Institutes of Health. Animals were allowed to acclimate for 7 days after receipt. They were group housed in accordance with institutional standards, received food and water ad libitum, and were maintained on a 12 h light/dark cycle. Male Sprague Dawley rats approximately 300−400 g in body weight were used. For time course studies, two animals per time point over three time points were used. For dose response studies, three animals per dose over 7−10 doses were tested. Animals were euthanized with carbon dioxide, and plasma and tissue removed. Tissue sections were prepared as previously described.[17]

■ ASSOCIATED CONTENT

Supporting Information

The Supporting Information is available free of charge on the ACS Publications website at DOI: 10.1021/acschemneuro.5b00303.

Analytical data and synthetic routes for compounds **5**−**7**, **9**, **11**, **12**, **20**−**24**, and **32**−**37** and experimental protocols for pharmacological assays, ADME and hERG assays (PDF)

■ AUTHOR INFORMATION

Corresponding Author

*E-mail: cchrovia@its.jnj.com.

Author Contributions

C.C. and M.L. conceived and oversaw the project series. A.S.-J. and C.C. conceived, synthesized and characterized final compounds. J.R. and G.B. conceived and synthesized intermediates. B.L. conducted receptor occupancy experiments. L.N. analyzed PK and receptor occupancy experiments. Q.W. and H.A. conducted P2X7 assays. M.L., A.B., and N.C. oversaw the project. C.C. drafted the manuscript. C.C. and A.S.-J. revised the manuscript.

Notes

The authors declare no competing financial interest.

■ ACKNOWLEDGMENTS

The authors would like to thank David Speybrouck for enabling chiral separations, Heather McAllister for HRMS data, and Warren Wade for optical rotation data.

■ REFERENCES

(1) Arulkumaran, N., Unwin, R. J., and Tam, F. W. K. (2011) A potential therapeutic role for P2X7 receptor (P2X7R) antagonists in the treatment of inflammatory diseases. *Expert Opin. Invest. Drugs 20*, 897−915.

(2) Stock, T. C., Bloom, B. J., Wei, N., Ishaq, S., Park, W., Wang, X., et al. (2012) Efficacy and safety of CE-224,535, an antagonist of P2X7 Receptor, in treatment of patients with rheumatoid arthritis inadequately controlled by methotrexate. *J. Rheumatol. 39*, 720−727.

(3) Keystone, E. C., Wang, M. M., Layton, M., Hollis, S., and McInnes, I. B. (2012) Clinical evaluation of the efficacy of the P2X7 purinergic receptor antagonist AZD9056 on the signs and symptoms of rheumatoid arthritis in patients with active disease despite treatment with methotrexate or sulphasalazine. *Ann. Rheum. Dis. 71*, 1630−1635.

(4) Donnelly-Roberts, D. L., and Jarvis, M. F. (2007) Discovery of P2X7 receptor-selective antagonists offers new insights into P2X7 receptor function and indicates a role in chronic pain states. *Br. J. Pharmacol. 151*, 571−579.

(5) For a review see: Chrovian, C. C., Rech, J. C., Bhattacharya, A., and Letavic, M. A. (2014) P2X7 antagonists as potential therapeutic agents for the treatment of CNS disorders. *Prog. Med. Chem. 53*, 65−100 see also references therein..

(6) Ali, Z., Laurijssens, B., Ostenfeld, T., McHugh, S., Stylianou, A., Scott-Stevens, P., Hosking, L., Dewit, O., Richardson, J. C., and Chen, C. (2013) Pharmacokinetic and phamacodynamic profiling of a P2X7 receptor allosteric modulator GSK1482160 in healthy human subjects. *Br. J. Clin. Phamacol. 75*, 197−207.

(7) Abdi, M. H., Beswick, P. J., Billinton, A., Chambers, L. J., Charlton, A., Collins, S. D., Collis, K. L., Dean, D. K., Fonfria, E., Gleave, R. J., Lejeune, C. L., Livermore, D. G., Medhurst, S. J., Michel, A. D., Moses, A. P., Page, L., Patel, S., Roman, S. A., Senger, S., Slingsby, B., Steadman, J. G., Stevens, A. J., and Walter, D. S. (2010) Discovery and structure−activity relationships of a series of pyroglutamic acid amide antagonists of the P2X7 receptor. *Bioorg. Med. Chem. Lett. 20*, 5080−5084.

(8) Jones, K. A., and Thomsen, C. (2013) The role of the innate immune system in psychiatric disorders. *Mol. Cell. Neurosci. 53*, 52−62.

(9) Thomas, A. J., Davis, S., Morris, C., Jackson, E., Harrison, R., and O'Brien, J. T. (2005) Increase in interleukin-1beta in late-life depression. *Am. J. Psychiatry 162*, 175−177.

(10) Owen, B. M., Eccleston, D., Ferrier, I. N., and Young, A. H. (2001) Raised levels of plasma interleukin-1beta in major and postviral depression. *Acta Psychiatr. Scand. 103*, 226−228.

(11) Iwata, M., Ota, K. T., and Duman, R. S. (2013) The inflammasome: Pathways linking psychological stress, depression, and systemic illnesses. *Brain, Behav., Immun. 31*, 105−114.

DOI: 10.1021/acschemneuro.5b00303
ACS Chem. Neurosci. 2016, 7, 490−497

(12) Csolle, C., Ando, R. D., Kittel, A., Goloncser, F., Baranyi, M., Soproni, K., Zelena, D., Haller, J., Nemeth, T., Mocsai, A., and Sperlagh, B. (2013) The absence of P2X7 receptors (P2rx7) on non-haematopoietic cells leads to selective alteration in mood-related behaviour with dysregulated gene expression and stress reactivity in mice. *Int. J. Neuropsychopharmacol. 16*, 213−233.
(13) Basso, A. M., Bratcher, N. A., Harris, R. R., Jarvis, M. F., Decker, M. W., and Rueter, L. E. (2009) Behavioral profile of P2X7 receptor knockout mice in animal models of depression and anxiety: relevance for neuropsychiatric disorders. *Behav. Brain Res. 198*, 83−90.
(14) Csolle, C., Baranyi, M., Zsilla, G., Kittel, A., Goloncser, F., Illes, P., et al. (2013) Neurochemical changes in the mouse hippocampus underlying the antidepressant effect of genetic deletion of P2X7 receptors. *PLoS One 8* (6), e66547.
(15) Iwata, M., Ota, K. T., and Duman, R. S. (2015) Psychological stress activates the inflammasome via release of ATP and stimulation of the P2X7 receptor. *Biol. Psychiatry*, DOI: 10.1016/j.biopsych.2015.11.026.
(16) Lovenberg, T., Aluisio, L., Ceusters, M., Letavic, M., and Bhattacharya, A. (2015) Characterization of P2X7 antagonists in the rodent brain: Promise for a novel mechanism of action for mood disorder? *Proceedings of the CINP Thematic Meeting on Stress, inflammation and depression: focus on novel antidepressant targets*, Dublin, Ireland, June 4−6, 2015, http://www.flipgorilla.com/p/2383741146944153/show#/2383741146944153/64.
(17) Hansen, K. B., Balsells, J., Dreher, S., Hsiao, Y., Kubryk, M., Palucki, M., Rivera, N., Steinhuebel, D., Armstrong, J. D., III, Askin, D., and Grabowski, E. J. J. (2005) First Generation Process for the Preparation of the DPP-IV Inhibitor Sitagliptin. *Org. Process Res. Dev. 9*, 634−639.
(18) Dean, D. K., Munoz-Muriedas, J., Sime, M., Steadman, J. G. A., Thewlis, R. E. A., Trani, G., and Walter, D. S. 5,6,7,8-Tetrahydro-[1,2,4]triazolo[4,3-a]pyrazine derivatives as P2X7 modulators. PCT Int. Appl. 2010, WO 2010125102 A1 20101104, November 2010.
(19) Rudolph, D. A., Alcazar, J., Ameriks, M. K., Anton, A. B., Ao, H., Bonaventure, P., Carruthers, N. I., Chrovian, C. C., De Angelis, M., Lord, B., Rech, J. C., Wang, Q., Bhattacharya, A., Andres, J. I., and Letavic, M. A. (2015) Novel methyl substituted 1-(5,6-dihydro-[1,2,4]triazolo [4,3-a]pyrazin-7(8H)-yl)methanones are P2X7 antagonists. *Bioorg. Med. Chem. Lett. 25*, 3157−3163.
(20) Savall, B. M., Wu, D., De Angelis, M., Carruthers, N. I., Ao, H., Wang, Q., Lord, B., Bhattacharya, A., and Letavic, M. A. (2015) Synthesis, SAR, and Pharmacological Characterization of Brain Penetrant P2X7 Receptor Antagonists. *ACS Med. Chem. Lett. 6*, 671−676.
(21) Hopkins, A. L., Groom, C. R., and Alex, A. (2004) Ligand efficiency: a useful metric for lead selection. *Drug Discovery Today 9*, 430−431.
(22) Hopkins, A. L., Keseru, G. M., Leeson, P. D., Rees, D. C., and Reynolds, C. H. (2014) The role of ligand efficiency metrics in drug discovery. *Nat. Rev. Drug Discovery 13*, 105−121.
(23) Deng, X., Liang, J., Allison, B. B., Dvorak, C., McAllister, H., Savall, B. M., and Mani, N. S. (2015) Allyl-assisted, Cu(I)-catalyzed azide-alkyne cycloaddition/allylation reaction: assembly of the [1,2,3]-triazolo-4,5,6,7-tetrahydropyridine core structure. *J. Org. Chem. 80*, 11003−11012.
(24) IC_{50} values are the mean of at least three experiments in triplicate, unless otherwise stated, h is human, r is rat, IC_{50} ± sd is reported.
(25) Bhattacharya, A., Wang, Q., Ao, H., Shoblock, J. R., Lord, B., Aluisio, L., Fraser, I., Nepomuceno, D., Neff, R. A., Welty, N., Lovenberg, T. W., Bonaventure, P., Wickenden, A. D., and Letavic, M. A. (2013) Pharmacological characterization of a novel centrally permeable P2X7 receptor antagonist: JNJ-47965567. *Br. J. Pharmacol. 170*, 624−640.
(26) Lord, B., Ameriks, M. K., Wang, Q., Fourgeaud, L., Vliegen, M., Verluyten, W., Haspeslagh, P., Carruthers, N. I., Lovenberg, T. W., Bonaventure, P., Letavic, M. A., and Bhattacharya, A. (2015) A novel radioligand for the ATP-gated ionchannel P2X7:[^{3}H] JNJ-54232334. *Eur. J. Pharmacol. 765*, 551−559.

DOI: 10.1021/acschemneuro.5b00303
ACS Chem. Neurosci. 2016, 7, 490−497